

c.2



Lawrence Berkeley Laboratory

UNIVERSITY OF CALIFORNIA

RECEIVED
LAWRENCE
BERKELEY LABORATORY

Materials & Molecular Research Division

JUN 3 1985

LIBRARY AND
DOCUMENTS SECTION

THE EFFECT OF H₂S AND COS IN THE FUEL GAS
ON THE PERFORMANCE OF AMBIENT PRESSURE
PHOSPHORIC ACID FUEL CELLS

P.N. Ross, Jr.

April 1985

TWO-WEEK LOAN COPY

*This is a Library Circulating Copy
which may be borrowed for two weeks.*



LBL-18001
c.2

DISCLAIMER

This document was prepared as an account of work sponsored by the United States Government. While this document is believed to contain correct information, neither the United States Government nor any agency thereof, nor the Regents of the University of California, nor any of their employees, makes any warranty, express or implied, or assumes any legal responsibility for the accuracy, completeness, or usefulness of any information, apparatus, product, or process disclosed, or represents that its use would not infringe privately owned rights. Reference herein to any specific commercial product, process, or service by its trade name, trademark, manufacturer, or otherwise, does not necessarily constitute or imply its endorsement, recommendation, or favoring by the United States Government or any agency thereof, or the Regents of the University of California. The views and opinions of authors expressed herein do not necessarily state or reflect those of the United States Government or any agency thereof or the Regents of the University of California.

The Effect of H₂S and COS in the Fuel
Gas on the Performance of Ambient Pressure
Phosphoric Acid Fuel Cells

Interim Report for Contract RP-1676-2

Philip N. Ross, Jr.
Principal Investigator
Materials and Molecular Research Division
Lawrence Berkeley Laboratory
Berkeley, CA 94720

Prepared for:

EPRI
3412 Hillview Avenue
Palo Alto, CA 94303

This research was supported by the Assistant Secretary for Fossil Energy, Office of Fuel Cells, Advanced Concepts Division of the U.S. Department of Energy under Contract No. DE-AC03-76SF00098, and by the Electric Power Research Institute under Contract No. RP-1676-2.

EXECUTIVE SUMMARY

The objective of this project was to determine in laboratory cells the tolerance of phosphoric acid fuel cells (PAFC) to hydrogen sulfide and carbonyl sulphide impurities in the anode feed gas. This objective arises from the interest in coupling fuel cells to coal gasifiers, and from the interest in expanding the fuel base for current PAFC technology to relatively heavy sulfur containing liquid fuels. EPRI supplied the compositions of three different coal gasifier effluent streams of interest to their coal gasifier/fuel cell program. These gas streams and their compositions are designated in Table I (see pg. 13 in text). For the purposes of this study, we simplified the compositions for the laboratory gases to hydrogen-carbon monoxide mixtures (balance nitrogen) containing various levels of hydrogen sulfide and carbonyl sulphide. Therefore, this study did not include the possibly additive negative effect of the other impurities (particularly the olefins) present in real coal gasifier effluent.

The study was conducted in three phases: the first was testing in a small (1 cm^2) free electrolyte cell to examine the effect of electrode structure on cell tolerance and to determine the "order of magnitude" of sulfur causing failure in cells at zero utilization; the second was testing in standard 2"x2" PAFC laboratory hardware at ambient pressure to examine the effect of hydrogen utilization on tolerance and the possible effect of fuel impurities on cathode performance; the final phase was testing with a 2"x2" cell in a pressure vessel to determine the effect of pressurized operation on cell tolerance.

The poisoning effect of hydrogen sulfide was characteristically different from the effect carbon monoxide, in that it was not manifested by a marginal (e.g. 0-50 mV) increase in anode potential but either had no effect or caused catastrophic polarization. Therefore, we derived critical levels for hydrogen sulfide as related to cell operating conditions. The poisoning effect of hydrogen sulfide was entirely an anode effect. The effect of carbonyl sulfide was complicated by the thermodynamic instability of COS in a hydrogen rich hydrogen-carbon monoxide gas mixture. We observed conversion of COS to hydrogen sulfide in our test cell by mass spectrometer analysis, but the kinetics of the hydrogenation of COS to H₂S could not be determined within the limitations of the study. Therefore, we recommend that the sum (total sulfur) be used as the criterion together with a specification on the hydrogen sulfide level.

Conclusions:

- 1.) Acceptable performance at electric utility operating conditions can be retained with (H₂S + COS) <50 ppm and H₂S <20 ppm provided CO levels are below ca. 2%.
- 2.) With respect to the EPRI gas compositions listed in Table I, Gas A is acceptable but neither B nor C is acceptable.
- 3.) Cell failure due to sulfur poisoning was irreversible, i.e. removal of the sulfur

impurity from the gas, did not alone restore performance.

4.) Failed cells can be restored by air purging in the "hot" state, or equivalently by clamping the anode to the cathode (after inert gas purging of the anode plenum).

5.) The critical level of sulfur was relatively insensitive to cell operating conditions near the region of interest, e.g. 50-120 psig, 190-205°C,

6.) A cell operating with a subcritical but significant (e.g. 10 ppm) level of H₂S exhibits greater sensitivity to temperature, i.e. greater V/ T.

1. Introduction

This task within our multiyear research project 1676-2 was initiated in September 1983 and the initial phase was identified as an approximately three month effort. In this initial phase, the objective was to determine which of the three proposed feed gases for a fuel cell anode shown in Table I would be acceptable for an ambient pressure cell. In the final phase, to be completed in CY1984, we will determine the effect of pressure, and pressurized conditions (acid concentration and temperature) on the tolerance of the cell to impurities in the anode feed gas. The particular impurities of interest in this study were the sulfur containing species, H_2S and COS . We further refined the criterion of "tolerance" of the cell to these impurities by using the determination of the critical level of either H_2S , COS or their sum¹ causing catastrophic failure of the cell, i.e. cell voltage drops precipitously to a very low value, 0-0.3 V. Because of the time constraints on this study, we could not determine the long term (1000 hr) effects of S species on cells that appeared tolerant by the above criterion, i.e. did not suffer catastrophic failure. Cells that did not suffer catastrophic failure upon introduction of subcritical S levels did run for several hundred hours without any apparent increase in the rate of decay over control cells.

The initial phase study was further divided into two segments: the first was testing in a small (1 cm^2) free electrolyte cell to examine the effect of electrode structure on cell tolerance and to determine the "order-of-magnitude" of S level causing failure in cells at zero utilization of hydrogen; the second segment was testing in standard 2" x 2" phosphoric acid fuel cell hardware with a fixed type of electrode to

examine the effect of utilization on cell and to determine the effect of anode impurities on cathode polarization. This latter point requires expanded consideration. Any fuel gas constituent which is not electrochemically oxidized at the anode can diffuse to the cathode, either directly by gas phase diffusion (there is always some cross-over in real cells in large stacks) or by diffusion through the electrolyte, and be adsorbed on the cathode catalyst. Because of the time delay due to the transport process, the time constant for the "cathode effect" is expected to be much longer than for the "anode effect." Due to the time constraints on this study, the "cathode effect" appeared to be problematic. However, we developed analytical techniques for detecting S species in the cathode gas which gave additional evidence as to the likelihood of significant "cathode effect" occurring in long-term testing.

2. Experimental

2.1 Gas Mixing System

Ten calibrated gas mixtures were used in this work as- received from Matheson. The compositions of these mixtures is given in Table II. The calibrated mixtures were blended in our laboratory manifold system to form the desired anode feed gas compositions. The gas manifold system is shown in Fig. 1. The flow controllers were calibrated for the specific gas controlled by the water displacement method. The total flow rate monitor for the anode gas was calibrated for a 33% H₂/67% N₂ mixture. The calibrations were done at gas flows corresponding to a hydrogen flow to the cell of ca. 20 (STP) min⁻¹, which is the hydrogen consumption rate

of a 25 cm² cell operating at 100 mA/cm². In comparison to the EPRI anode gas compositions A-C the only significant variation in major constituents between those in Table III and those in Table I is the absence of CO₂ in the LBL feed gas. Previous testing in our laboratory had shown that CO₂ had no effect on fuel cell anodes other than a dilution effect (1), so the CO₂ was replaced with N₂ to simplify gas mixing and calibration.

The composition of gases in the anode was checked periodically by gas sampling and analysis with a mass spectrometer (Balzers Model 100). This procedure was also applied to the cathode gas vent, and proved to be a useful way to detect H₂S or other S species diffusing across the cathode.

2.2 Test Cell Design

Two sizes and types of cells were used. The first was a small (1 cm²) free-electrolyte cell of LBL design which was used to determine the effect of electrode structure on S level tolerance. The small cell permitted a large number of electrodes to be prepared and testing with relatively small amounts of catalyst, PTFE and SiC being consumed. Once a particular type of electrode was selected for further study, the critical S level was determined without hydrogen utilization in the small cell (shown in the photograph in Fig. 2.). The final determination of the critical S level was made using the selected electrodes in the 2" x 2" standard phosphoric acid subscale test hardware (2). This cell had a SiC matrix, with the SiC applied to the electrode at LBL. Due to difficulties we had in preventing "cross-over" of hydrogen in our cells, the matrix was much thicker than in commercial cells, resulting in a much higher resistance (ca. 5 times higher) than is usual practice.

2.3 Electrodes

The catalysts used in both the anode and cathode were the same, 10% Pt on

Vulcan XC-72 R carbon black purchased from Prototech Company. This catalyst was the colloid type described in the patents of Petrow and Allen (3). Cathodes were fabricated on Stackpole PC-206 graphite substrates using the techniques described in a previous EPRI report (4). Anodes were also fabricated at LBL on Stackpole PC-206 using variable PTFE content and curing temperatures; in addition we tested anodes supplied to us by Prototech (designated K-105) which were designed for use in their zinc electrowinning cells. We found that the Prototech K-105 electrodes produced better S tolerance in the cell than any of the LBL fabricated anodes. In addition, the Prototech electrodes were supplied in the 2" x 2" size which we could use directly in the 2" x 2" hardware; we did not have capability to fabricate 2" x 2" electrodes at the start of this study. Therefore, all results reported here were obtained using the Prototech K-105 anodes.

2.4 Test Procedure

Slightly different test procedures were used in the 1 cm² cell and the 2" x 2" cell. In the 1 cm² cell, polarization curves were obtained using a PAR 173D Potentiostat/Galvanostat operated in the constant current (galvanostatic) mode. The IR drop between electrodes was measured by current interruption. At start-up, the cell was filled with H₃PO₄ pre-concentrated to 98 w/o after pre-heating the dry cell to ca. 100° C. The cell was heated to ca. 180° C and left exposed to air on both electrodes for 15-18 hrs. The anode was flushed with N₂, then switched to pure H₂; the cathode gas was switched directly to pure O₂. This established the time zero condition of the cell in all tests. On the 2" x 2" cell, the start-up procedure was identical, but the discharge of the cell was achieved using a solid-state load (Acme Electronics, SSL-500).

The total cell resistance was measured in the air-open circuit state using an AC impedance bridge (ESI Model 253) at 1 kHz. No attempt was made to break down the cell resistance into component parts.

Composition analysis of either the anode or cathode vent gas was conducted periodically by flowing the vent gas through a 100 ml glass sampling bulb. The sampling bulb was then transferred to the mass spectrometer for elemental analysis. Only the H₂S or SO₂ concentrations were measured, as the CO (in cathode gas) could not be resolved from the N₂. Quantitative cell calibration was achieved by using N₂/H₂S (or N₂/SO₂) peak ratios from calibrated gas mixtures. In general, the mass spectrometer determined H₂S levels in the anode gas vent were within $\pm 10\%$ of the value expected from the flow controller calibrations. Because of the limited time period for this study, we did not have the opportunity to develop procedures for COS analysis owing to its more complex cracking pattern.

3. Results

3.1 H₂S Effects

The effect of H₂S on the 1 cm² cell voltage at 100 mA/cm² CO is shown in Fig. 3. Addition of 90 ppm H₂S resulted in almost instantaneous failure. Monitoring of the anode and cathode potentials versus an external reference electrode indicated the polarization increase was exclusively at the anode in this time frame. Removing the H₂S from the anode gas stream did not restore cell voltage. That the H₂S and CO have a coupled effect was shown by removing the CO then adding it back; the cell voltage dropped back to its fully poisoned value, also indicating the adsorbed S

species never left the Pt surface. Performance could only be restored to the GM-2B level by O_2 activation (i.e. burn-off), which consisted of flushing the anode with N_2 , then with O_2 for 10 min., then returning to GM-2B. In this sequence, the cell also failed at 19 ppm H_2S at the 2% CO level. However, with duplicate electrodes it was observed that if the cell were first put on GM-3B it ran for a few hundred hours with no increase in the rate of decay over that for a control (i.e. GM-2B). Apparently not all the adsorbed S was removed from the Pt surface during the O_2 activation applied in that sequence. We did not have the opportunity to investigate this irreversibility phenomena in greater detail, so its not clear what chemistry is truly responsible for the lasting effect of high H_2S exposure.

The effect of H_2S on cell voltage with 1% CO is shown in Fig. 4. In this case the cell ran without significant loss on 19 ppm H_2S , but failed rapidly when the level increased to 47 ppm H_2S . Also unlike the failed cell in Fig. 3, the O_2 activation restored performance on GM-3A, the H_2S containing gas as well as GM-2A, the CO containing H_2S - free gas. Dropping the temperature from 180 C to 160 C while running on GM-3A had a small (ca.-20mV) effect on cell voltage that was about the same as the temperature effect on GM-2A.

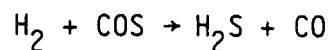
It was clear from the 1 cm^2 cell tests that the critical level of H_2S in a cell running without utilization of H_2 was between 19 and 47 ppm. A curious feature of H_2S poisoning (curious in the sense that it differs from the behavior with other poisons like CO) is that we never observed incremental effects of H_2S on anode polarization, i.e. the effect was either minimal or catastrophic. This is the rationale behind experimental design aimed at determining critical levels of H_2S , since the behavior of

cells with H₂S displays this go/no-go characteristic. The effect of H₂ utilization of the critical level of H₂S, and the longer time behavior of cells running with H₂S, are shown in Fig. 4. Reducing the anode gas flowrate through the 2" x 2" cell to a rate where 80% of the H₂ is consumed at 100 mA/cm² caused a 25-30 mV decrease in cell voltage. Switching from GM-2B to GM-3B with 19 ppm H₂S produced no change in cell voltage over a 50 hr. period. Increasing the H₂S level to 47 ppm (GM-4B) produced catastrophic failure. Similar results were obtained with the A-series (1% CO) gases. We concluded from the 2" x 2" cell tests with 80% H₂ utilization the critical H₂S level appeared to be between 19 and 47 ppm H₂S, as observed in the 1 cm² cell without H₂ utilization.

The effect of H₂S on cell voltage was observed at two other current densities, 50 and 200 mA/cm². The results were identical to those observed at 100 mA/cm², indicating that the critical level of H₂S causing cell failure is not particularly sensitive to the current density (within the practical range).

3.2 COS Effect

The COS effect was complicated by the thermodynamic instability of COS in a H₂-rich H₂/CO mixture. The appropriate thermochemical data are given in Table IV. The hydrogenation of COS



to H₂S has a negative standard free energy of reaction and is mildly endothermic, meaning that increasing temperature will shift the equilibrium even further to the right. At 200°C, the equilibrium constant is 20.3. For a gas containing 33% H₂ and 1-2% CO, the equilibrium

conversion at 200°C of COS to H₂S is essentially 100%. We observed the conversion of COS to H₂S in our cell with the mass spectrometer, but it was not complete conversion and we did not have the time to carry out a detailed study of the kinetics of this conversion. It seems likely that on the Pt catalyst surface in the anode, local equilibrium is achieved so that to the surface an H₂/CO/COS gas and an H₂/CO/H₂S gas are equivalent. The observations of cell behavior on COS indicate that this simple analysis has some validity. In Fig. 4, the effect of COS with and without H₂S is shown. Adding COS to GM-2B at the 50 ppm level had virtually no effect when the cell was running without H₂ utilization, but when the gas flow slowed to the rate for 80% H₂ utilization the cell began to decay but with a time constant that was much longer than that for 47 ppm H₂S. It is not clear what this difference in time effect means, and the 0% utilization cell response to 50 ppm COS was very different from that for 47 ppm H₂S (cell failure). It could be that COS hydrogeneration is occurring both in the gas lines and within the anode catalyst layer, but local equilibrium is not achieved at the Pt surface, so that the effective gas composition at the Pt surface is some unknown COS/H₂S ratio. Blending the H₂S and COS gases, instead of producing H₂S only by COS hydrogeneration, produced a cell response that also indicated that the mixture of H₂S + COS is not as deleterious as the equivalent S level as H₂S, since the cell ran for more than 250 hrs. on 19 ppm H₂S + 25 ppm COS but failed with 47 ppm H₂S. These results suggest that COS is not itself a poison for H₂ oxidation, but has an indirect effect by virtue of its hydrogeneration to H₂S (which is a poison) in mixtures like those used in fuel cell anodes. However, until more detailed studies of H₂S + COS mixtures and COS chemistry are conducted, it is recommended that the

sum total be used as a guideline, i.e. ($\text{H}_2\text{S} + \text{COS}$) 50 ppm and 20 ppm.

3.3 Cathode Effects

Monitoring the individual electrode potentials against an external hydrogen reference electrode indicated that on the time scale of these tests (<1000 hrs.) the poisoning by S species was entirely at the anode. This leaves open the question of whether there might be long-time effects at the cathode due to slow diffusion of S species through the matrix to the cathode catalyst surface. We addressed this question in two ways. First, we estimated the time constant for the diffusion process from the diffusion equation,

$$C = C_0 \operatorname{erfc} [x/2(Dt)^{1/2}]$$

assuming a 0.1 cm matrix and a diffusivity for H_2S equal to that for H_2 (5). The time constant is ca. 3 hrs. Secondly, we measured the time required for H_2S to appear in significant concentrations in the cathode gas upon introduction of H_2S into the anode gas, and found that it was less than 15 hrs (overnight). Thus, if there were cathode effects due to S species in the anode gas they should have manifested themselves within the time period of our observations.

There are other observations indicating that S species do not affect the cathode polarization. The air/ O_2 activation procedure, that apparently "burns-off" the S surface species, is equivalent to raising the potential of a poisoned anode to the potential of the air/ O_2 electrode, and one should expect then rapid oxidation of S species rather than adsorption and accumulation on the surface. In what we referred to as cell failure in discussing Figs. 3-5, the cell voltage did not actually go to zero (or

below) but to an impractically low voltage. The "poisoned" cell was actually running at a quasi-steady voltage of 0.25-0.3 V, with the anode at + 350-400 mV versus RHE. The voltage was quasi-steady in the sense that there were regularly periodic oscillations in voltage, which we postulated were related cyclic oxidation of S species and readsorption (6). This was confirmed qualitatively by mass spectroscopic analysis of the anode gas which showed SO_2 was produced during this oscillatory behavior. SO_2 was never observed in the anode gas under any other condition of operation of the cell. It seems reasonable to conclude that S species diffusing to the cathode from the anode gas are rapidly oxidized to inert SO_2 without poisoning the Pt surface for O_2 reduction.

4. Discussion

There are very few studies of sulfide adsorption on Pt that are relevant to the particular circumstances of the phosphoric acid fuel cell anodes. Most studies (7,8) of sulfide adsorption on Pt have been at room temperature in dilute acid, not in concentrated H_3PO_4 at high temperature as here. There was a previous study of H_2S poisoning of fuel cell anodes conducted by UTC for EPRI and reported in EM-1328. Our results are consistent with some of the results in that study, and at variance with others. They conducted tests on pressurized and non-pressurized (atmospheric pressure) cells; their simulated adiabatic reformer effluent (anode feed) gas composition was somewhat more dilute in hydrogen than that used here, 20% H_2 , 1.7% CO , 31% CO_2 , 47% N_2 . In agreement with our findings, they reported relatively rapid cell failure with 50 ppm H_2S in both pressurized and atmospheric cells. They did not report tests at

lower H_2S levels than 50 ppm, so they made no conclusions as to what level of H_2S an anode would be tolerant. At variance with our findings is the reported reversibility of H_2S decay, and an apparent "clean-off" effect of CO. They reported that adding 100 ppm H_2S to the simulated reformer gas caused rapid (failure in <2 hrs.) decay, and removal of H_2S from the fuel stream resulted in a performance recovery symmetric with the decay. We never observed this reversible behavior; as described above, removal of H_2S from the fuel gas did not restore performance, only "burn-off" restored anode performance. It is not clear why in tests which are apparently so similar in materials and procedure such dissimilar behavior should be observed. However, there was concurrence in the practically important observation that neither pressurized nor atmospheric cells will run with 50 ppm H_2S in anode feed gas from an adiabatic reformer. In addition, our work has shown that atmospheric pressure cells will run on adiabatic reformer gas with ($H_2S + COS$) <50 ppm provided H_2S 20 ppm. The UTC report properly emphasized the lack of understanding of the mechanism of H_2S (or COS) poisoning of anodes. Cell testing of the kind done here, and previously at UTC, cannot provide the kind of understanding needed to predict the behavior of anodes with sulfur impurities. Since there is some promise that anodes can run on levels of H_2S and COS of practical interest, it is recommended that detailed studies of H_2S (and related molecule) adsorption on Pt be conducted in the manner done previously by Stonehart and co-workers (9,10) for CO on Pt. Such studies should probably proceed, or at least be conducted in parallel, expanding testing of 2" x 2" hardware or stacks on sulfur containing fuels.

5. Conclusions

5.1 Relative to the EPRI proposed anode feed gas compositions in Table I, subscale hardware testing at atmospheric pressure has indicated that:

- o Gas A is acceptable
- o Gas B is unacceptable
- o Gas C is unacceptable

5.2 Anodes are more tolerant to COS than to H₂S, but it is recommended that the sum (total sulfur) be used as a criterion. On this basis it appears that acceptable performance can be retained with (H₂S + COS) <50 ppm provided H₂S <20 ppm.

5.3 Sulfur poisoning is entirely an anode effect.

5.4 Sulfur poisoning is irreversible, i.e. removal of the source does not alone restore performance.

5.5 Sulfur poisoned anodes can be reactivated by either "hot" air exposure or, equivalently, by clamping the anode to the cathode (after N₂ purging the anode).

5.6 The critical (H₂S + COS) level is relatively insensitive to current density in the 50-200 mA/cm² range.

5.7 The critical (H₂S + COS) level is relatively insensitive to temperature in the 160-180°C range.

Table I. EPRI Proposed Feed Gases.

Component	Gas A	Gas B	Gas C
H ₂	35	35	35
CO ₂	25	25	25
N ₂	36	34.5	30.4
H ₂ O	1.6	1	1
Impurities			
CH ₄	1	2	5
CO	1	2	3
argon	0.4	0.5	0.6
C ₂ H ₄	100 ppm	500 ppm	1000 ppm
** C ₂ ⁺	100	1000	4000
Cl ₂	2	5	10
* H ₂ S	4	50	100
* COS	2	50	100
** NH ₃	1	50	100
** HCN	1	5	10

* Primary importance

** Secondary importance

Table II. Matheson Calibrated Gas Mixtures.

<u>Mixture</u>	<u>Composition</u>
N ₂ /CO	1.5% CO bal. N ₂
	3.0% CO bal. N ₂
	6.0% CO bal. N ₂
H ₂ /H ₂ S	57 ppm H ₂ S bal. H ₂
	141 ppm H ₂ S bal. H ₂
	271 ppm H ₂ S bal. H ₂
N ₂ /COS	500 ppm COS bal. N ₂

Table III. Anode Gas Feed Compositions.

<u>Notation</u>	<u>Composition (dry basis)</u>
GM-1	100% H ₂
GM-2A	33% H ₂ , 66% N ₂ , 1% CO
GM-3A	33% H ₂ , 66% N ₂ , 1% CO, 19 ppm H ₂ S
GM-4A	33% H ₂ , 66% N ₂ , 1% CO, 47 ppm H ₂ S
GM-5A	33% H ₂ , 66% N ₂ , 1% CO, 90 ppm H ₂ S
GM-2B	33% H ₂ , 66% N ₂ , 2% CO
GM-3B	33% H ₂ , 65% N ₂ , 2% CO, 19 ppm H ₂ S
GM-4B	33% H ₂ , 65% N ₂ , 2% CO, 47 ppm H ₂ S
GM-5B	33% H ₂ , 65% N ₂ , 2% CO, 90 ppm H ₂ S
GM-2C	33% H ₂ , 64% N ₂ , 4% CO

Table IV. Thermochemical Data.[†]

Species	ΔG_f^{298} (kcal/mol)	ΔH_f^{298} (kcal/mol)	ΔG_f^{500} (kcal/mol)
COS	-39.6	-33.1	-43.73
H ₂ S	-8.0	-4.9	-9.6
CO	-32.8	-26.4	-37.14
H ₂ + COS → H ₂ S + CO	-1.2	+1.8	-3.01

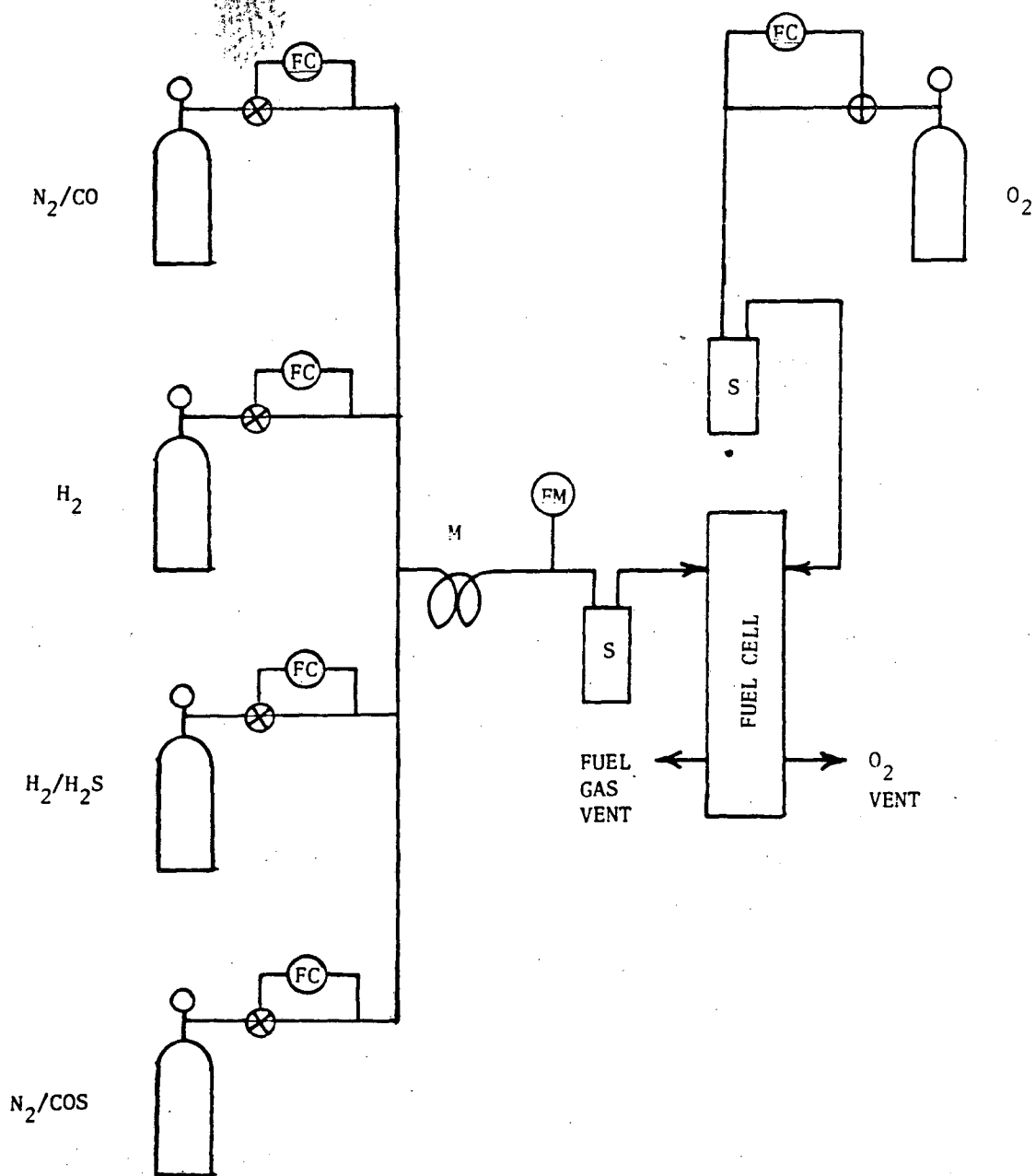
[†]JANAF Thermochemical Tables, 2nd. Edition, 1971.

References

- 1.) P.N. Ross, J. Electrochem. Soc., 130, 882 (1983).
- 2.) Design follows that used by Energy Research Corp., Danbury, CT.
- 3.) H. Petrow and R. Allen, U.S. Patent 3,992,512, Nov. 16, 1976.
- 4.) P.N. Ross, EPRI Report EM-1553, Sept. 1980.
- 5.) K. Klinedinst, J. Bett, J. MacDonald and P. Stonehart, J. Electroanal. Chem., 57, 281 (1974).
- 6.) Pourbaix gives the standard potential for $\text{H}_2\text{S} \rightarrow \text{S} + 2\text{H}^+ + 2\text{e}^-$ as 0.142 V and for $\text{S} + 2\text{H}_2\text{O} \rightarrow \text{SO}_2 + 4\text{H}^+ + 4\text{e}^-$ as 0.451 V. Sulfide on the surface can be regarded thermodynamically as underpotential sulfur (elemental).
- H₂S — 7.) N. Ramasubramanian, J. Electroanal. Chem., 64, 21 (1975).
- 8.) E. Najdeker and E. Bishop, J. Electroanal. Chem. 41, 79 (1973).
- 9.) W. Vogel, J. Lundquist, P. Ross and P. Stonehart, Electrochim. Acta, 20, 79 (1975).
- CO — 10.) P. Stonehart and P.N. Ross, Electrochim. Acta, 21, 441 (1976).

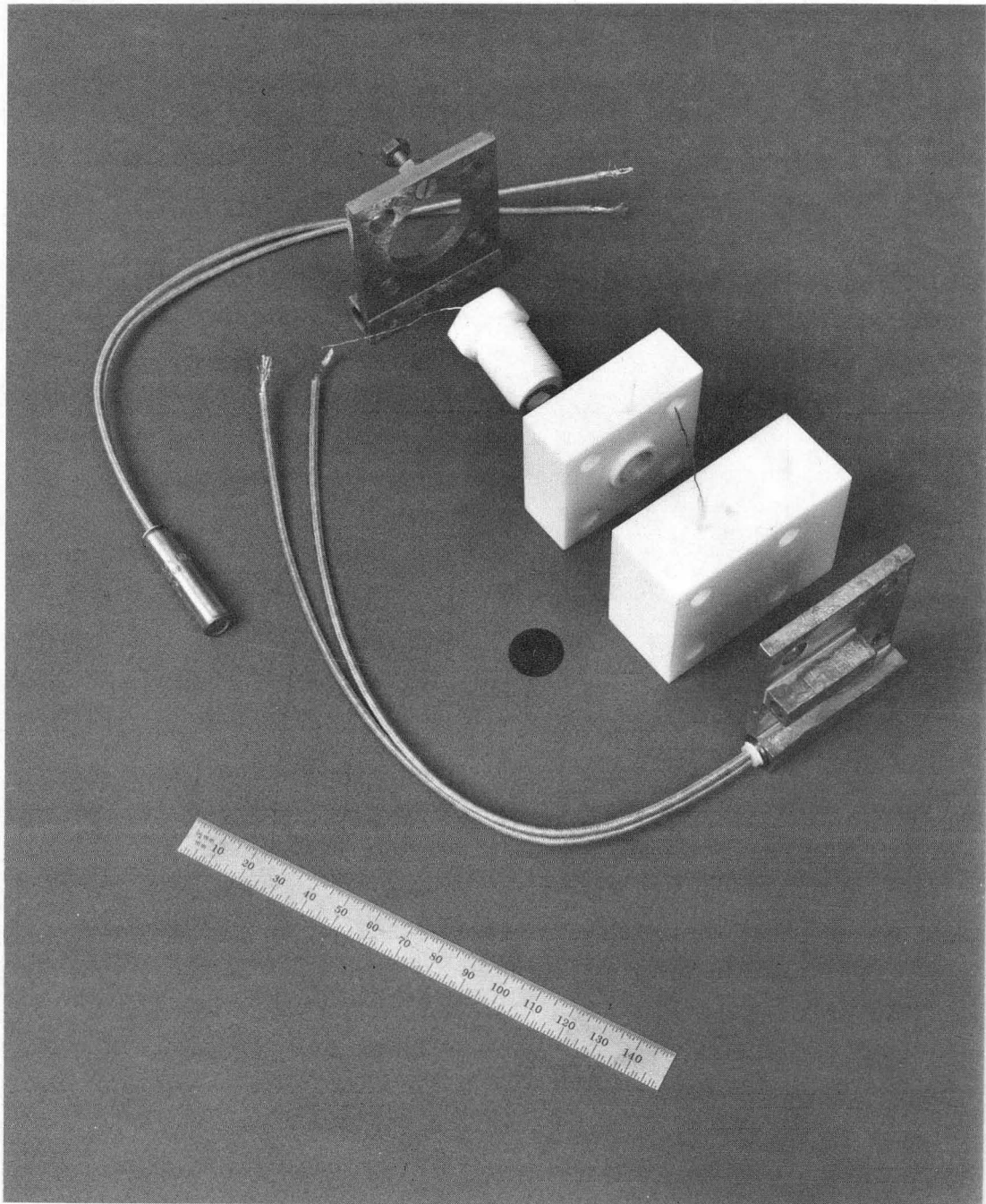
Figure Captions

- Figure 1. Schematic diagram of gas mixing manifold for blending the calibrated gases listed in Table II to form the fuel gas mixtures listed in Table III. Symbols: FC - flow controller; FM - flow monitor; M - mixing loops; S - water vapor saturators. (XBL 846-2246)
- Figure 2. Photograph of the 1 cm² fuel cell used for evaluation of sulfur effects at zero utilization. (XBB 845-3873)
- Figure 3. Effect of H₂S in fuel gas stream on 1 cm² cell voltage at 100 mA load current. 180°C, 98 w/o H₃PO₄. (XBL 843-10118)
- Figure 4. Repeat of run in Fig. 2 with new electrodes but starting at the lowest H₂S level studied here. (XBL 843-10117)
- Figure 5. Effect of H₂S and COS in fuel gas stream on a 25 cm² cell at 2.5 A load current with and without utilization of the H₂. 180°C, 98 w/o H₃PO₄. (XBL 843-10119)



XBL 846-2246

Fig. 1



XBB845-3873

Fig. 2

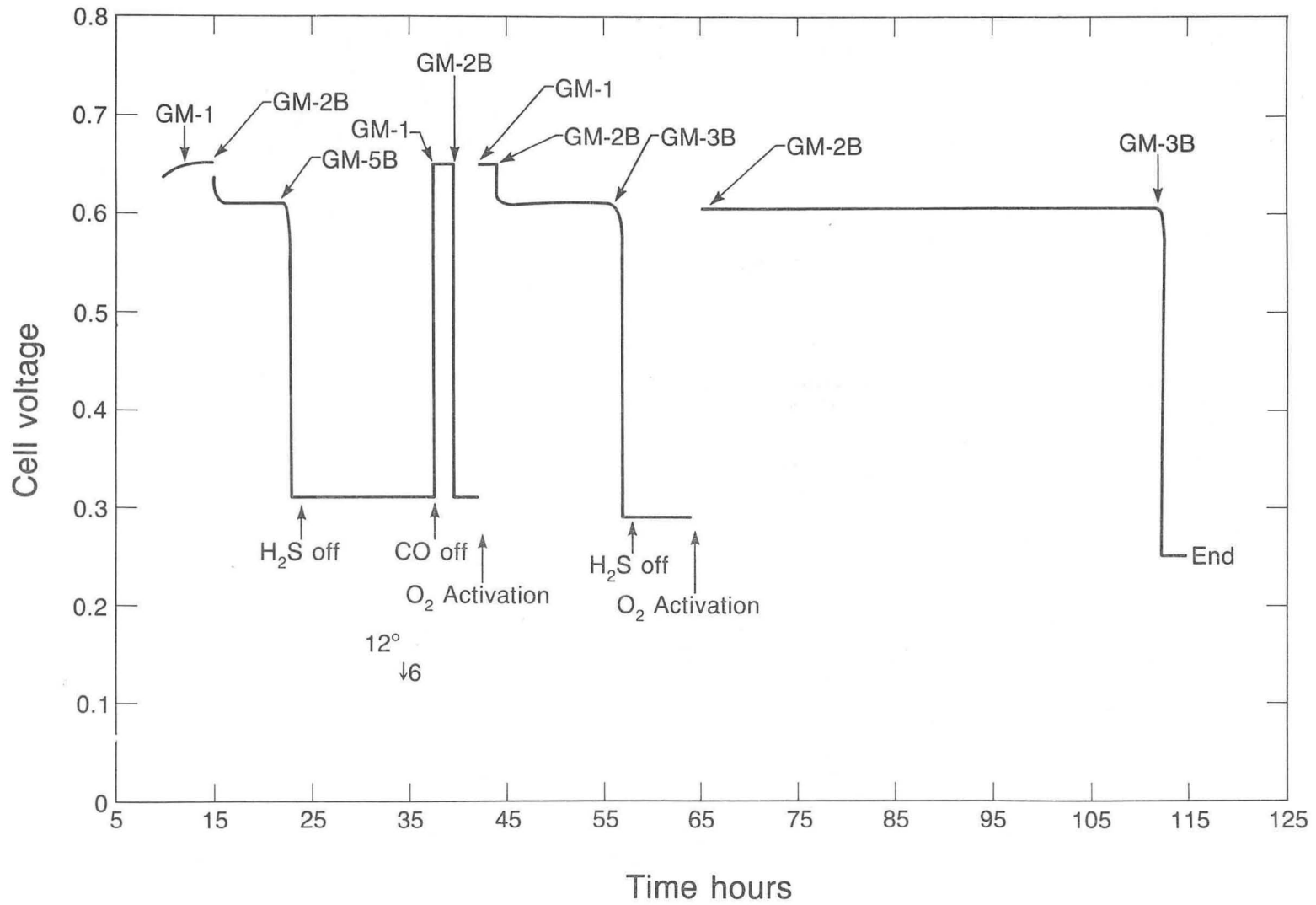


Fig. 3

XBL 843-10118

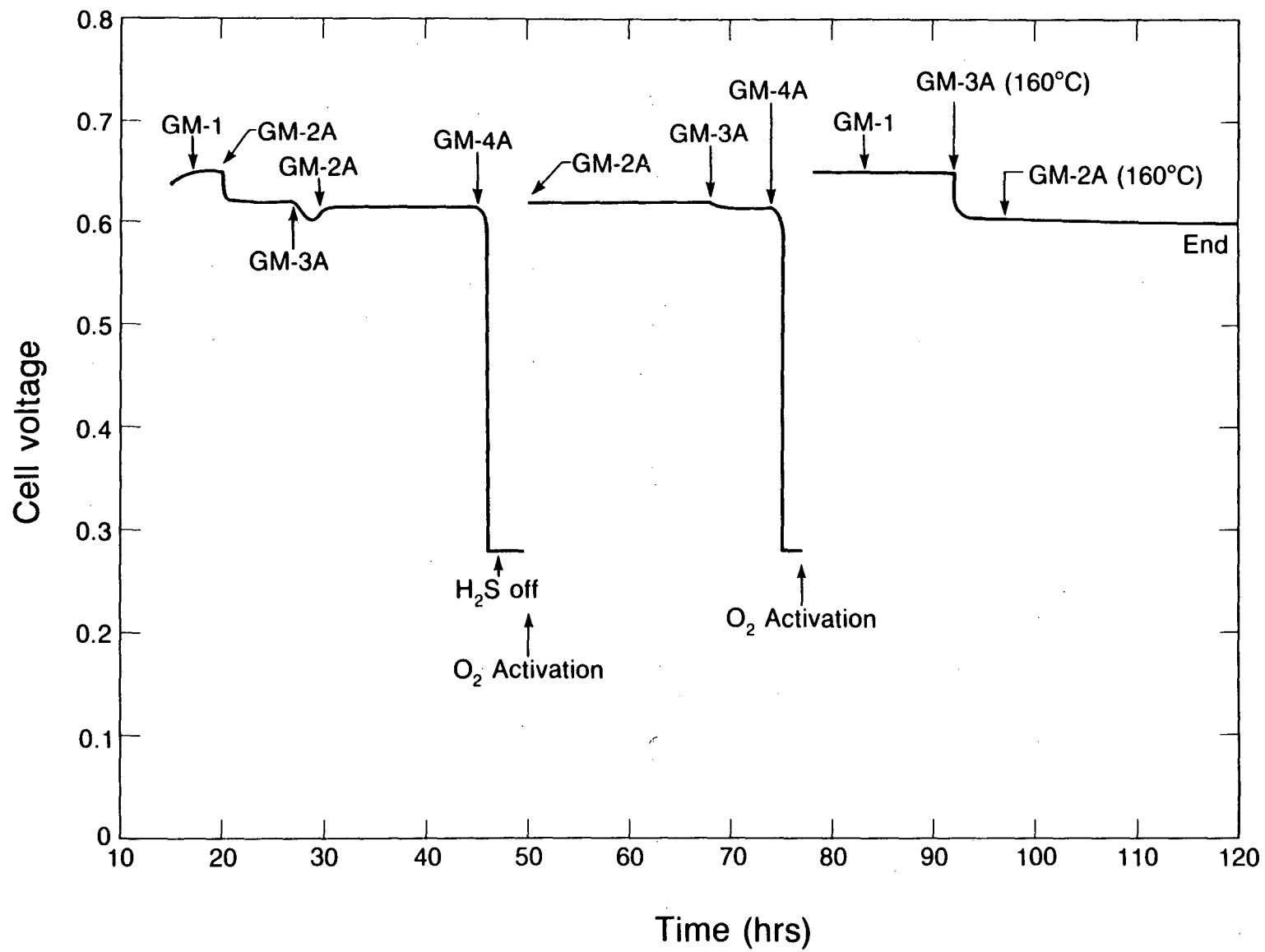


Fig. 4

XBL 843-10117

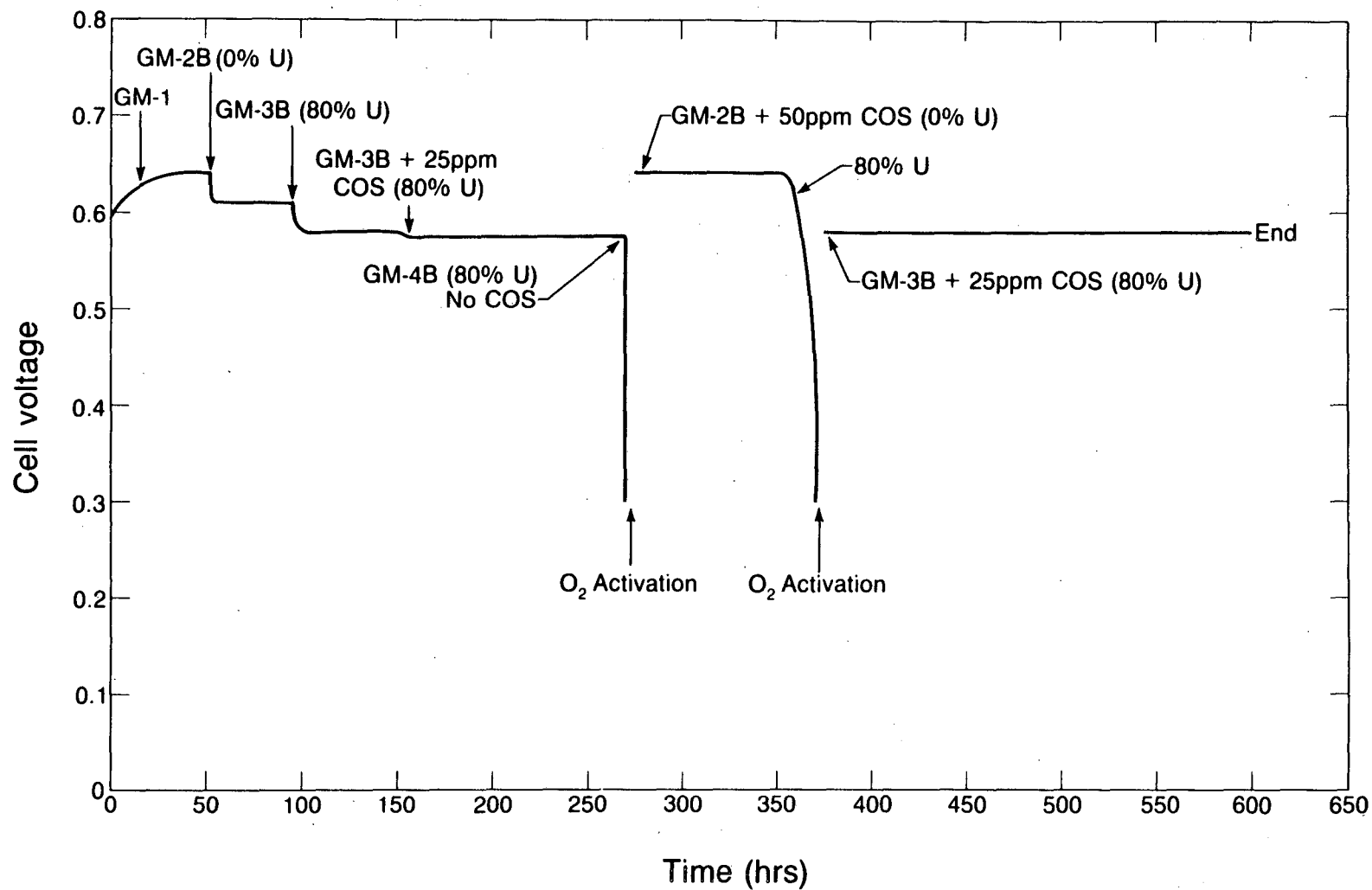


Fig. 5

XBL 843-10119

ADDENDUM TO EPRI STUDY ON THE EFFECT OF
H₂S AND COS ON PHOSPHORIC ACID FUEL CELLS

Anode Tolerance to H₂S and COS at Electric
Utility Operating Conditions (Pressurized)

1. Introduction

Following the completion of the ambient pressure study, which was described in the first section of this report, we proceeded to the third and final phase of the study, which was the determination of the effect of pressure and pressurized conditions (acid concentration and temperature) on the tolerance of the cell to impurities in the anode feed gas. At the request of EPRI, we narrowed the range of H₂S and COS concentrations to levels within the acceptable limits as indicated by the ambient pressure data, and determined the pressure-temperature relation on cell tolerance within this range. This also simplified the gas manifolding for the pressurized test stand, and reduced the cost of the study. The gas mixing train shown in Fig. 1 was eliminated, with a single gas composition used for the contaminated feed, 13 ppm H₂S, 20 ppm COS, 1% CO, 35% H₂, balance nitrogen. From safety and cost considerations, it was decided to use H₂-H₂ cells, rather than H₂-O₂ cells, since the ambient pressure data had indicated that sulfur poisoning was an entirely anode effect.

2. Experimental

The manifolding schematic for the pressurized test stand is shown in Fig. 6. The pressure vessel was fabricated from heavy-walled 316 stainless-steel 4.5 inch i.d. tubulation and contained the 2"x2" cell used in the ambient pressure study. The external reference electrode was a stationary (vs. flowing H₂) hydrogen electrode connected to the SiC matrix via a Ta capillary. The graphite endplates were machined to contain an electrolyte reservoir to assist in buffering differential pressure between the reference electrode chamber and the common gas chamber of the pressure vessel. The differential pressure gauge was an ITT Barton Gauge with a 316 stainless-steel bellows, 0-30 inch H₂O differential pressure readout with a precision of 1.0 inches. The free electrolyte volume in the reservoir and reference electrode was sufficient to provide a + 2.0 inches acid differential pressure. A schematic of the cell and reference electrode is shown in Fig. 7. The cell contained identical standard fuel cell type Pt on Vulcan carbon electrodes, Prototech K-105, 0.32 mg Pt/cm². The anode gas feed passed across the back of the anode and into the pressure vessel, then exited through a vent valve into the ambient (fume hood). No gas was forced across the back of the cathode (hydrogen evolving); the grooves in the end plate for this electrode were open to the common gas space of the pressure vessel. Thus, the cathode was also exposed to the feed gas impurities. The reference electrode was sealed in pure hydrogen at the same pressure as the gas in the pressure vessel. The anode polarization was determined galvanostatically using a DC current supply and by reading

the anode potential versus the reference electrode with a high input impedance digital voltmeter. Since the tip of the Luggin capillary was pressed against the SiC matrix on the cathode side, the anode potential reading included the potential drop across the matrix, which was determined by measuring the total cell resistance with an AC impedance bridge (ESI Model 253) at H_2 - H_2 open circuit. The total cell resistance for these builds was typically about 50 milliohms. The open circuit potentials for the anodes were always within a few tenths of an eV of the values calculated from the Nernst equation using the known gas compositions and assuming an equilibrium water vapor content in both the anode and reference gases, e.g. at 120 psig, 205 C, 96% acid the Nernst value is 16.2 mV vs. 17 mV measured. Hydrogen utilization (fraction of hydrogen in feed gas consumed electrochemically) was controlled by changing the anode feed gas rate with a pre-calibrated micrometer-head metering valve and monitoring with a pre-calibrated rotameter on the ambient pressure side of the cell vent valve.

Anode feed gases were derived from two calibrated mixtures, one the basic CO- H_2 mixture, 1% CO, 35% H_2 , bal. N_2 , and the basic mixture with 13 ppm H_2S . COS was added using a permeation tube with a permeation rate such that at the gas flowrate for 80% hydrogen utilization the COS level in the gas stream would be 20 ppm.

2. Results

The basic steady-state operating conditions for the testing of cell tolerance was 205 C with 95% acid at 120 psig and a current density of 325 mA/cm². At this basic operating condition, **the anode polarization was found to be totally unaffected by the presence of 13 ppm H₂S and 20 ppm COS in the feed gas.** This tolerance was observed at utilizations up to 80%; higher utilizations were not explored. Kitagawa detector tubes were used to determine that the gas exiting the cell had approximately the expected level of sulfide throughout the time span of the test, i.e. to be certain the sulfide was not being scavanged by some part of the gas manifold. The cell tolerance was observed continuously for a time span of 100 hrs. Longer term testing was not conducted and did not appear warranted in the context of this study.

Following the observation of cell tolerance at the basic operating condition, we explored the sensitivity of the tolerance to variations in operating conditions, specifically, to variations in pressure, temperature and current density. Fig. 8 shows the effect of thermal cycling a cell with and without H₂S (at zero utilization) in the feed at the basic conditions of pressure and current density. The presence of H₂S caused the rate of loss of anode potential with temperature (i.e. the dV/dT) to be somewhat greater than for a CO-H₂ feed. If we use 20 mV as the "acceptable" voltage loss, then the "critical" temperature for cell tolerance is slightly higher with the H₂S present, but at no point in the temperature cycle did we observe the catastrophic and irreversible

polarization that characterized poisoning in the ambient pressure cell (at 50 ppm H₂S).

At lower pressure, 80 psig, the dV/dT during the temperature cycle was much steeper, and the "critical" temperature was about 5 degrees higher, than at 120 psig, as shown by a comparison of the curves in Figs. 8 and 9. The effect of utilization at 120 psig was similar to lowering the pressure, as indicated by the curve in Fig. 10. Lowering the current density from 325 to 200 mA/cm² at 120 psig lowered both dV/dT and the "critical" temperature, as seen from the curve in Fig. 11. At 200 mA/cm², the difference due to H₂S is hardly discernable from the CO effect.

COS appeared to have no effect on any of the results reported in Figs. 8-11. However, we did not have independent measurement of the COS level in the gas stream, so it is not certain what the level was in these tests. If the permeation tube installation was working according to specifications, the level would have been 10-20 ppm.

3. Conclusions

Phosphoric acid fuel cells with standard Pt on Vulcan XC-72R catalyst (at 0.32 mg/cm²) are tolerant to fuel gases containing ca. 10 ppm H₂S and 10-20 ppm COS at nominal pressurized operating conditions of 190-210 C, 95% acid, 120 psig, 80% hydrogen utilization at 325 mA/cm² (or lower).

Figure Captions

Fig. 6. Schematic diagram of the pressurized cell manifolding and gas regulation.

Fig. 7. Schematic diagram of the 2x2 cell and reference electrode configuration in the pressure vessel.

Figs. 8-11. Temperature cycling tests of the effect of CO and CO plus H₂S on anode potential (uncorrected for IR drop across matrix). Conditions as indicated.

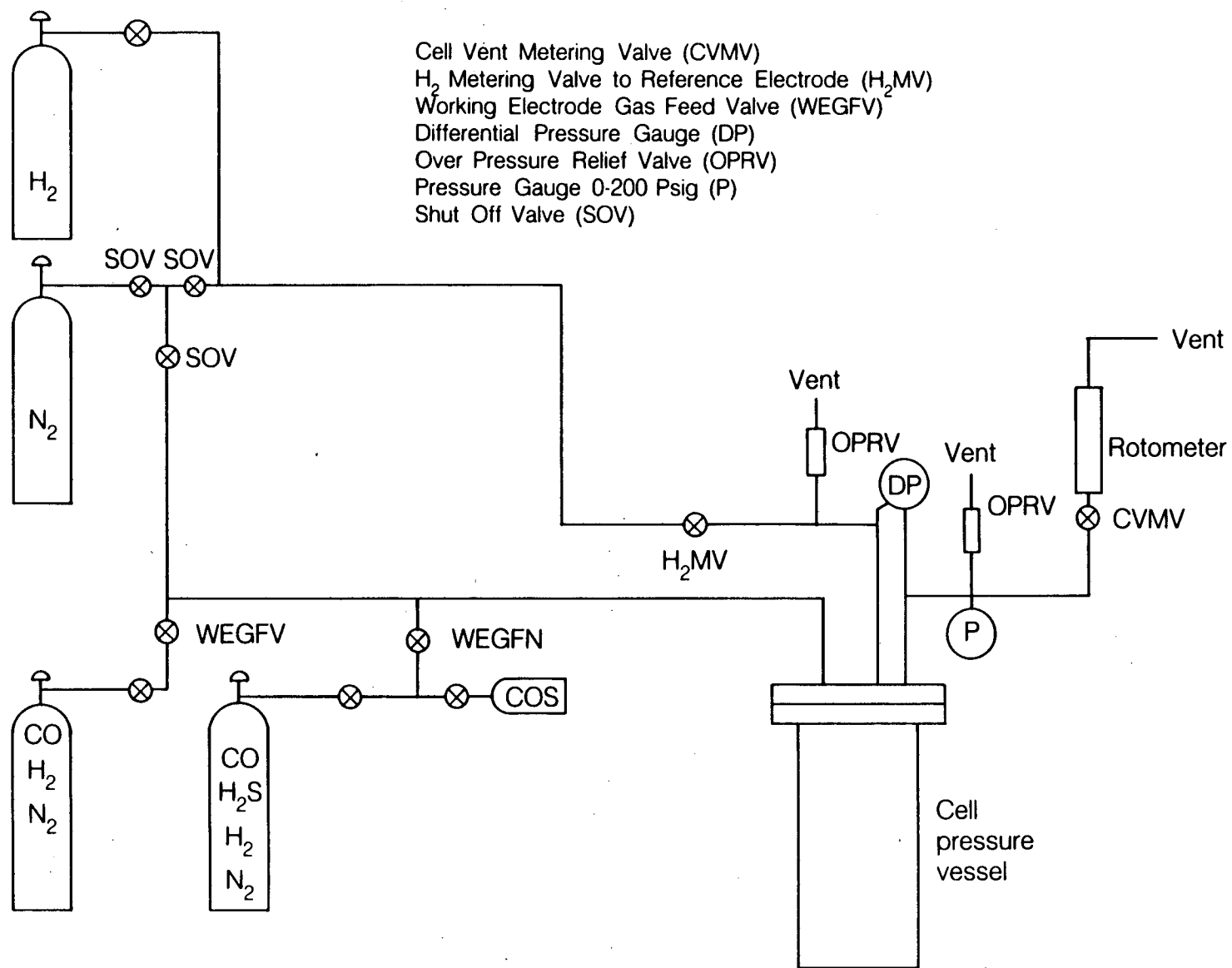
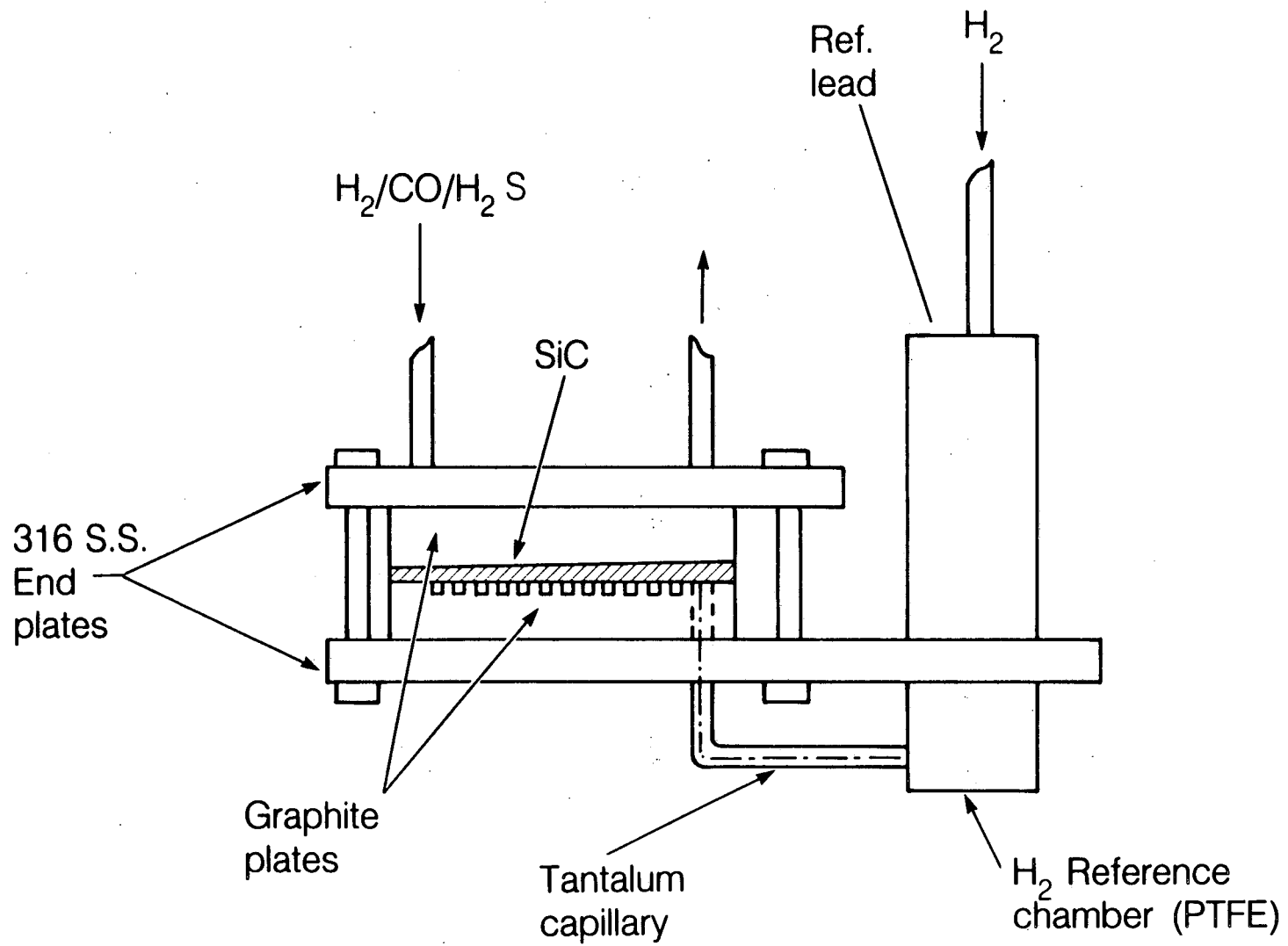


Fig. 6

XBL 853-10150



XBL 853-10147

Fig. 7

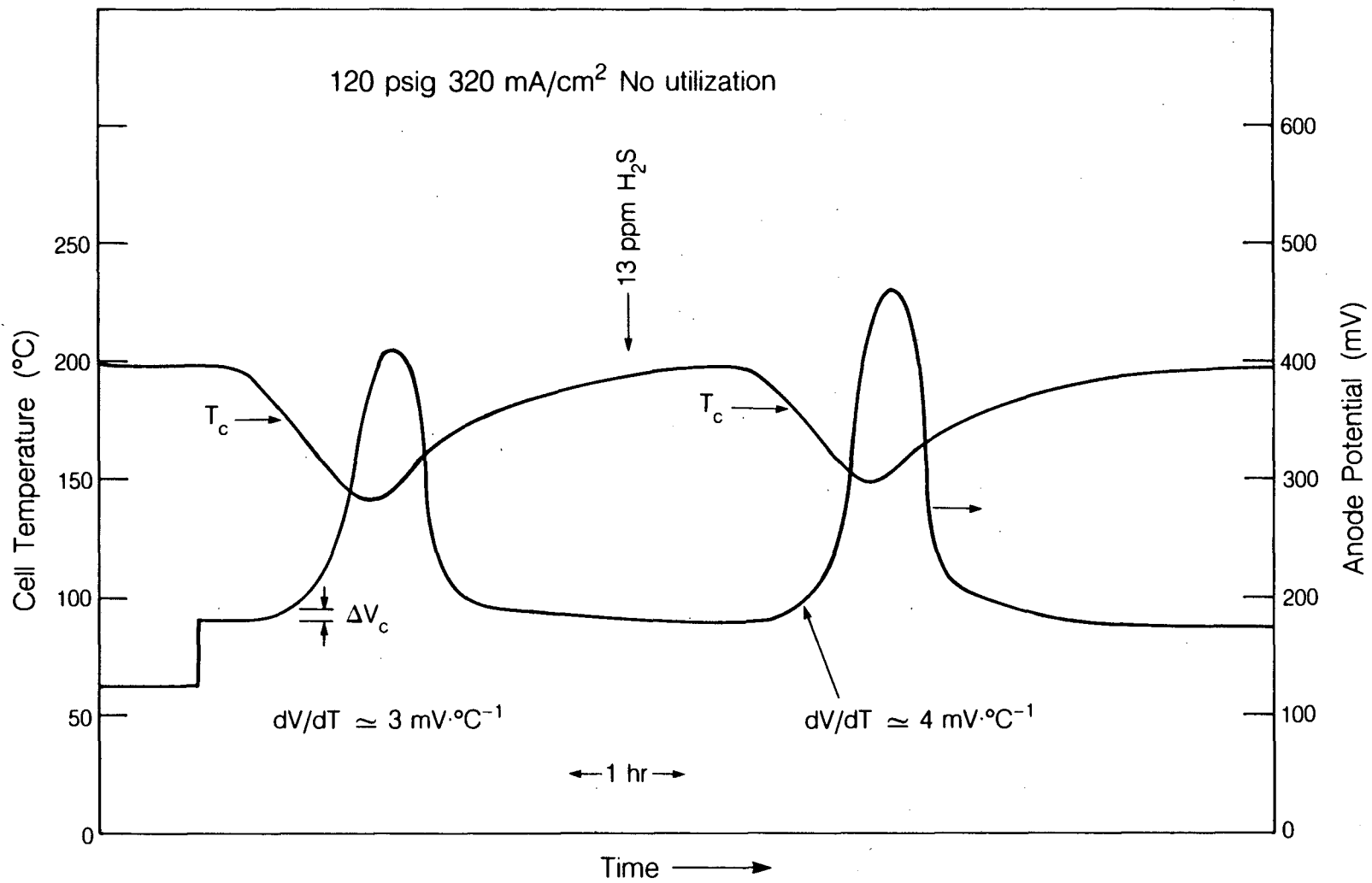
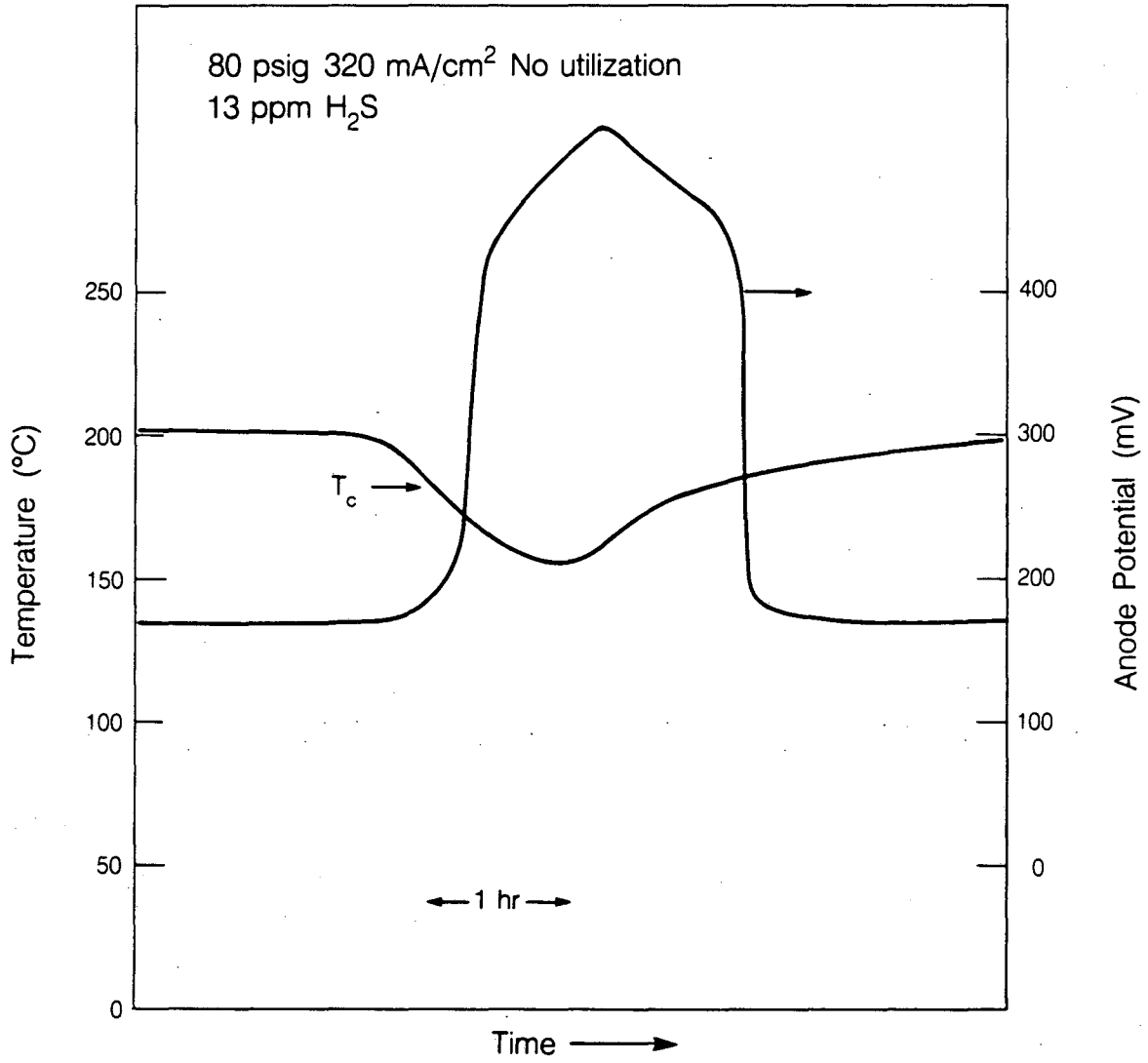
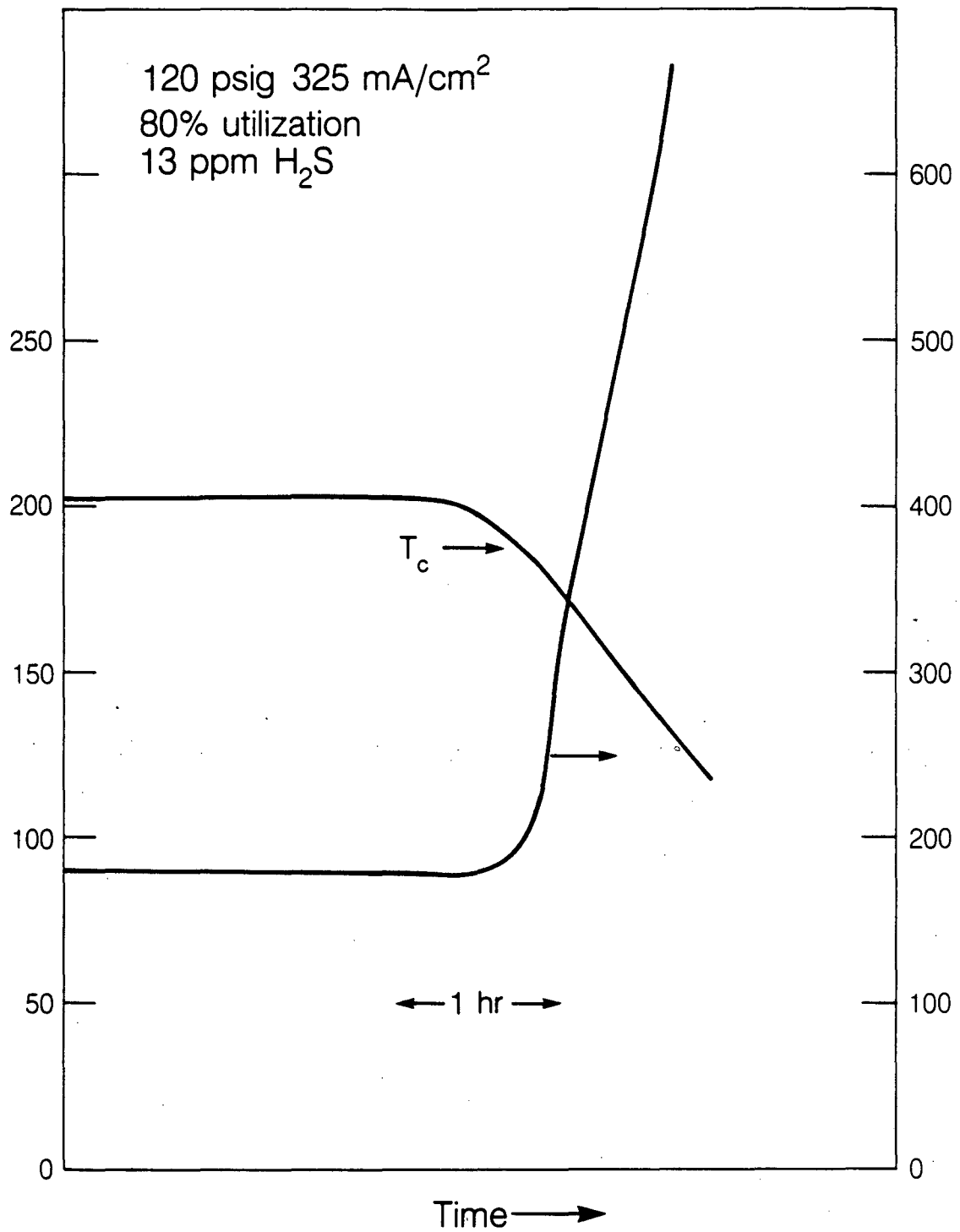


Fig. 8



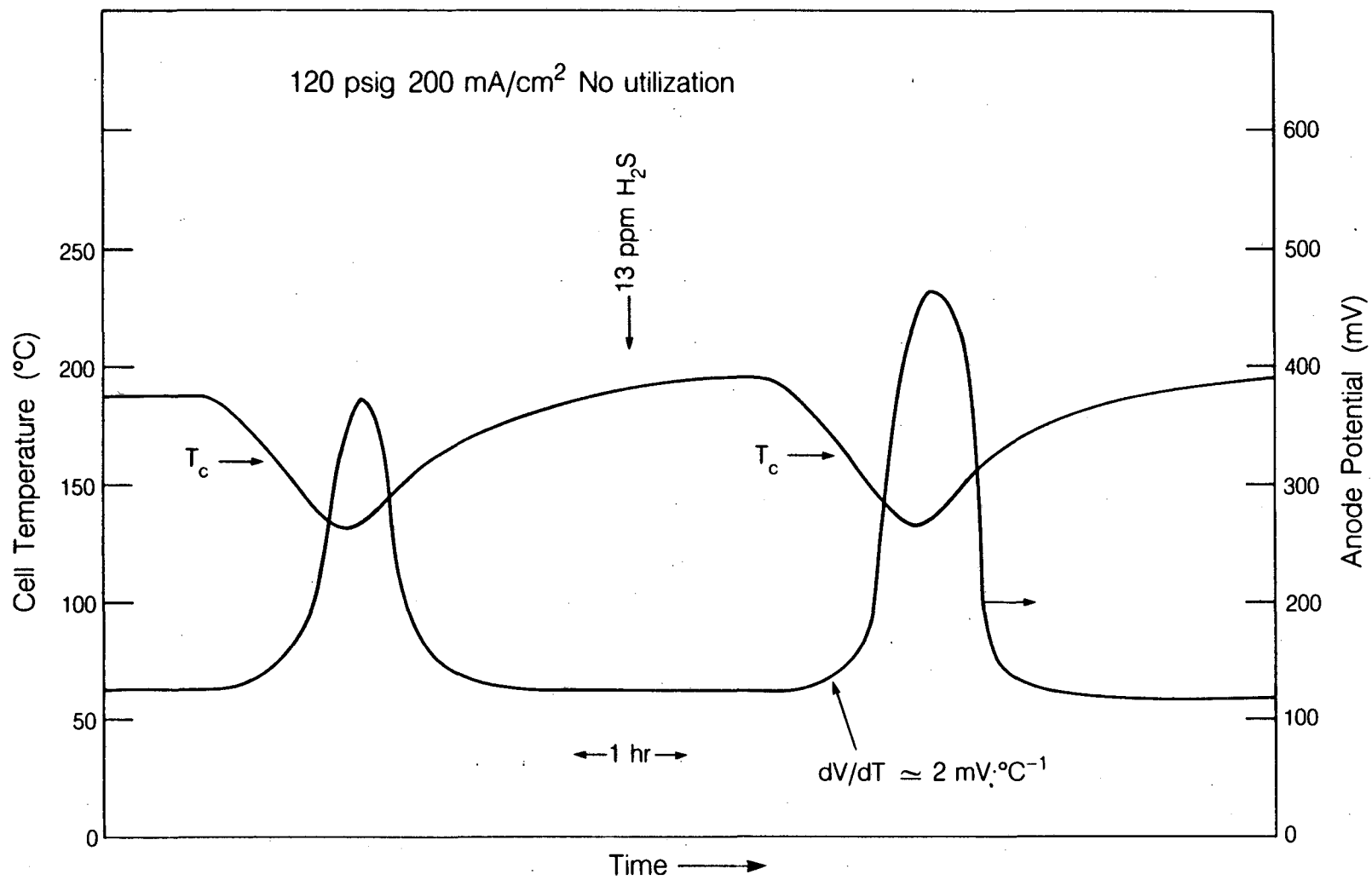
XBL 853-10148

Fig. 9



XBL 853-10149

Fig. 10



XBL 853-10151

Fig. 11

This report was done with support from the Department of Energy. Any conclusions or opinions expressed in this report represent solely those of the author(s) and not necessarily those of The Regents of the University of California, the Lawrence Berkeley Laboratory or the Department of Energy.

Reference to a company or product name does not imply approval or recommendation of the product by the University of California or the U.S. Department of Energy to the exclusion of others that may be suitable.

*LAWRENCE BERKELEY LABORATORY
TECHNICAL INFORMATION DEPARTMENT
UNIVERSITY OF CALIFORNIA
BERKELEY, CALIFORNIA 94720*